

STUDY OF TRANSPORT AND TRAPPING IN Sb_xSe_{1-x} ALLOYS

V.I.Mikla, Yu.Yu.Nagy, V.V.Mikla and A.V.Mateleshko

Institute for Solid State Physics & Chemistry, Voloshina Str. 54, 294000 Uzhgorod, Ukraine

Effect of antimony addition is clearly manifested in the electrical behavior of glassy selenium. Analysis of the trapping of photoinjected carriers and of the thermal generation of free carriers in the bulk reveal that in Sb_xSe_{1-x} alloys each of these processes is mediated by a specific manifold of localized electronic states residing in the mobility gap. The present observations clearly establish that the population of these states increases progressively with Sb content.

Introduction

There is both a scientific and technological interest in studying the transport/trapping of drifting electrons and holes in a-Se [1,2]. The application of the conventional time-of-flight and newly developed xerographic experiments for determining charge carrier lifetimes (releasetimes) in various a-Se alloys has contributed to both understanding and characterizing the effect of alloying a-Se [1-8].

In the present paper, we report the effect of antimony on the deep states of selenium. These states are the thermal emission (trapping) centers which control the slow dark decay, first and cycled-up residual potential of the surface voltage on capacitively charged specimen films.

Experimental details and procedure

Sample preparation

Amorphous films of Sb_xSe_{1-x} ($0 \leq x \leq 0.05$) system were prepared by the flash evaporation technique. Glassy Sb-Se alloy source material was made by conventional melt quenching. The cleaned silica tubes containing the mixture of the appropriate amount of constituents Sb and Se were evacuated to 10^{-5} Torr and sealed. The contents of the tubes were melted in a furnace and continuously agitated for 10 h to ensure good homogeneity. The melt was rapidly quenched in cold water from 800 K and cooling rate was estimated to be 200 K s^{-1} .

The Sb_xSe_{1-x} alloy was then vacuum deposited onto an aluminium substrate. The substrate was cleaned in neutral detergent, deionized water, ethyl alcohol, acetone and then oxidized in air at 1800°C before deposition.

Deposition of the Sb_xSe_{1-x} alloys were performed at a substrate temperature of 300 K. The thickness of the film was controlled to 20 μm . Prior to measurements, the Sb_xSe_{1-x} films prepared were aged for 2-3 weeks to allow for their physical properties to equilibrate.

Experimental procedure

The electrophotographic properties of the samples were measured using conventional xerographic technique. The sample is charged to a potential V_0 by passing it under corotron device that deposits charges of appropriate sign on the surface of the film. The surface potential is then measured by a transparent probe and an electrostatic voltmeter. The photoreceptor, the corona charging units and a transparent probe were housed in a well-shielded and dark environment. Following the initial charging process, the sample is exposed to strongly absorbed 450 nm step illumination from a tungsten light source during which time the decay of the surface electrostatic potential is monitored by the electrostatic voltmeter. The surface potential decays to a potential V_r (termed the residual potential) and the resulting photoinduced discharge curve (PIDC) can be used to determine the xerographic photosensitivity of the sample. The above xerographic step could be repeated any number of times to obtain a cycled-up residual surface potential V_m as a function of the xerographic cycle n .

Results and Discussion

There are essentially three important types of xerographic behaviour, generally termed the dark discharge, first cycle residual, and the cycled-up residual voltage, which must be considered in evaluating the electrophotographic properties of pure a-Se and its alloys.

The three xerographic properties of Sb_xSe_{1-x} are considered in the following.

Dark discharge

Typical dark discharge characteristics for pure Se and Sb_xSe_{1-x} photoreceptors are shown in Fig.1 for compositions noted in the figure. It is apparent that for pure a-Se the decay of the surface potential is relatively slow. Comparison of the respective characteristics for a- Sb_xSe_{1-x} with the dark discharge behaviour of pure a-Se shows clearly that alloying a-Se with antimony increases the dark decay rate.

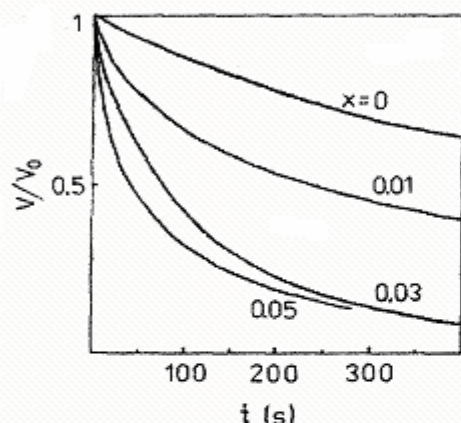


Fig.1. Dark discharge of surface potential on a- Sb_xSe_{1-x} layers. The surface potential at time t is normalized to that at $t=0$ (initial charging potential; $V_0=260$ V).

The discharge rates in a- Sb_xSe_{1-x} were not constant but decreased with time. There are a number of physical processes which can lead to the decay of the surface potential. The presently accepted model for the dark decay in a-Se-based films is that which involves [1,9,10]:

surface generation and injection of trapped electrons and their consequent transport across the sample substrate injection bulk thermal generation of carriers of one sign and depletion.

With relatively thick films ($L=10-50$ μm) and a good blocking contact between a-Se-based films and the preoxidized Al substrate the latter phenomenon dominates.

In a series of experiments carried out on a composition series of glassy Sb_xSe_{1-x} alloys it was found that the time dependent dark decay rate of the potential to which a dark rested film has been charged is controlled by the de-

pletion discharge process. In general, the xerographic depletion discharge model is based on bulk thermal generation involving the ionization of a deep mobility gap center to produce a mobile charge carrier of the same sign as the surface charge and an oppositely charged ionic center [9,10]. Assuming negative charging, a mobile electron would be thermally generated and the ionized center would be positive. As thermally generated holes are swept out by the electric field, a positive bulk space charge builds up with time in the specimen, causing the surface potential to decay with time.

Typical dark discharge data for Sb_xSe_{1-x} exemplifies the predicted of depletion discharge behavior. Inflections in the log-log plots at the respective depletion times are readily identifiable. Some special problems can, however, complicate the observation of a depletion kink in pure a-Se. The dark discharge rate was typically so slow in a-Se that results were always perturbed by injection. The central reason for pure Se possessing good dark decay characteristics is (1) the relatively low ($\sim 10^{13}$ cm^{-3}) concentration of deep localized states in the mobility gap of a-Se, and (2) the energy location of these states is deep ($E_t \sim 0.9-1.0$ eV) in the mobility gap, so that the thermal generation process of carriers from these centres is slow [1, 2, 4, 10].

It is found that in a- Sb_xSe_{1-x} alloys electrons (the mobile carrier species) are depleted (n-type system) during dark decay leaving behind a deeply trapped positive space charge. Note that the same situation prevails in alkali-doped a-Se [11].

Photoinduced discharge characteristics

In essence, the xerographic photosensitivity (S) of a photoreceptor material determines the rate of decay, dV/dt , of the electrostatic surface potential of the samples during photoinduced discharge. The xerographic photosensitivity definition adopted here is simply based on the amount of light energy required for the surface potential to decay to half of its original value ($V_0/2$) during photoinduced discharge (i.e. the fractional change in the surface potential per unit light exposure).

Only electrons are mobile in a- Sb_xSe_{1-x} (in the range of compositions studied), with a

drift mobility that is only slightly field dependent and nearly 1-2 orders of magnitude smaller than in a-Se. Consequently, the photoinduced discharge in a-Sb_xSe_{1-x} photoreceptors is controlled mainly by bulk transport.

Fig.2 shows a dark decay curve and a photoinduced discharge curve for a-Sb_{0.03}Se_{0.97} film. It can be seen that the sample exhibits relatively little dark decay. Nevertheless, to take into account the surface charge reduction during illumination and to evaluate S accurately, the contribution of dark discharge to the total change in the surface potential during PID was subtracted ($V_0 - V_d$ in Fig.2).

The xerographic spectral response for both a-Sb_{0.03}Se_{0.97} and pure Se are shown in Fig.3. It is apparent that as Sb is added to a-Se, the photosensitivity at a particular wavelength increases. More precisely this means that the xerographic photosensitivity for Sb_xSe_{1-x} alloy is somewhat greater at longer wavelengths ($\lambda > 670$ nm) than for pure Se, and smaller at shorter wavelengths ($\lambda < 500$ nm). Note that other compositions of Sb-Se alloy showed similar trends. The fact of increased xerographic photosensitivity of Sb-Se alloy at longer wavelengths suggests that the addition of antimony to a-Se causes a reduction of the band gap of the material.

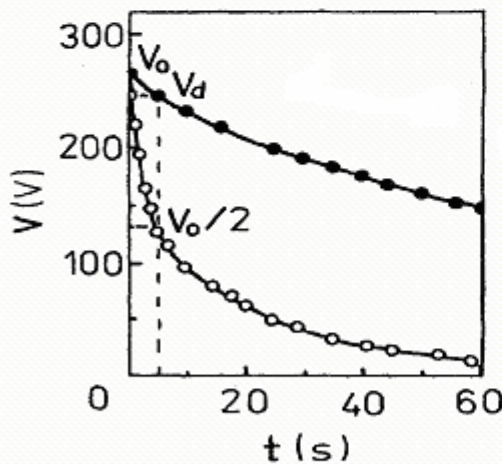


Fig.2. Dark decay curve (solid circles) and photoinduced discharge curve (open circles) for Sb_{0.03}Se_{0.97}.

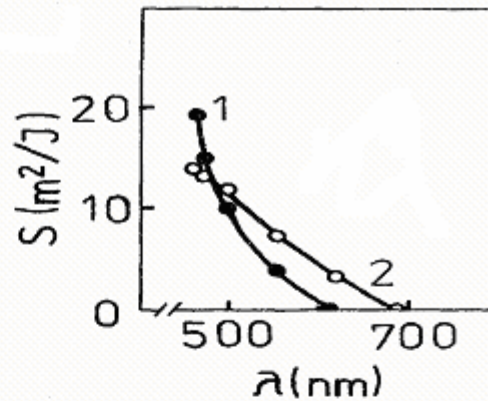


Fig.3. Xerographic photosensitivity (S) versus exposure wavelength (λ) for pure Se (1) and Sb_{0.03}Se_{0.97} (2) alloy films. For all measurements, the light intensity (I) was kept constant at $0.7 \text{ J m}^{-2} \text{ s}^{-1}$ and the electric field was kept at $E = 2.3 \times 10^5 \text{ V cm}^{-1}$.

For the films under examination the residual voltage V_r (a measurable surface potential at the end of the illumination) increases with Sb content (Fig.4). The residual potential is due to trapped electrons in the bulk of specimen. The simplest theoretical model which is based on range limitation and weak trapping ($V_r \ll V_0$) relates V_r to $\mu\tau$ (the drift mobility, μ , and lifetime, τ , product) via the Warter equation [12] $V_r = L^2 / (2 \mu \tau)$ where L is the sample thickness. For example, addition of 3at.% Sb leads to a change in the first cycle residual voltage from 4 to 44 V which is equivalent to a change of the carrier range, $\mu\tau$, from 10^{-7} to $10^{-6} \text{ cm}^2/\text{V}$. Substituting $\mu^e \sim 5 \times 10^{-3} \text{ cm}^2/(\text{V s})$ for pure Se and $\mu^e \sim 6 \times 10^{-4} \text{ cm}^2/(\text{V s})$ for Sb_{0.03}Se_{0.97} into the corresponding equation we find carrier lifetimes $\tau \approx 2 \times 10^{-4} \text{ s}$ and $\tau \approx 1.3 \times 10^{-3} \text{ s}$ in a-Se and a-Sb_{0.03}Se_{0.97}. It is necessary to note here that in general, bulk deep trapping lifetimes computed from the first cycle residuals are in agreement with lifetimes measured in the time-of-flight mode under range-limited conditions.

Fig.5 displays the buildup of the residual voltage V_m on an a-Sb_{0.03}Se_{0.97} film with the number of xerographic cycles n. The rate of increase in V_m with n decreases as cycling increases, until eventually for large n (≥ 6 in our case) V_m tends to a saturated value V_{rs} .

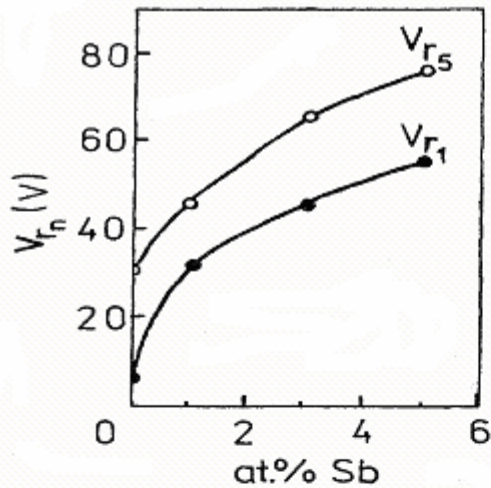


Fig.4. Effect of antimony on the residual potential (measured after first and fifth cycles) of Sb-Se alloy.

As described earlier [13], the saturation residual potential provides an experimental measure of the integrated number of deep traps (trap-release rates are much slower than those from shallow traps which control drift mobility). V_{rs} is then simply given by

$$V_{rs} = eN_t L^2 / (2\epsilon)$$

where N_t is the deep-trap concentration and ϵ is the dielectric constant.

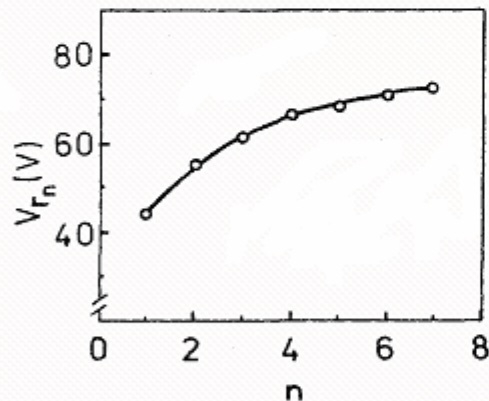


Fig.5. The build-up in the residual voltage with number of xerographic cycles in a-Sb_{0.03}Se_{0.97}

REFERENCES

1. S.O.Kasap. In: The handbook of imaging materials. Marcel Dekker, New York, 1991.
2. L.Cheung, G.M.T.Foley, P.Furnia and B.E.Springett, *Photogr. Sci. & Eng.*, 26 (1982) 245.
3. J.Schottmiller, M.Tabak, G.Lucovsky and
8. V.I.Mikla, *Phys. Stat. Solidi B* 182 (1994) 325.
9. A.R.Melnyk, *J. Non-Cryst. Solids* 35/36 (1980) 837.
10. M.Abkowitz, F.Jansen and A.R.Melnyk, *Phil. Mag. B* 51 (1985) 405.
11. M.Abkowitz and F.Jansen, *J. Non-Cryst.*

films. One charge-discharge cycle consists of 60 s light decay with a 1000 lx tungsten lamp after corona charging.

Both the first residual and the cycled-up saturated residual potential are sensitive to alloying. For example, when pure amorphous Se films are alloyed with antimony, the buildup of the residual potential occurs more rapidly toward a much higher saturated residual potential. We obtain, for instance, $N_t \sim 2 \times 10^{14} \text{ cm}^{-3}$ and $N_t \sim 10^{15} \text{ cm}^{-3}$ for a-Se and Sb_{0.03}Se_{0.97}, respectively.

The exact way in which charge transport and trapping are controlled in a-Sb_xSe_{1-x} is not well understood. Nevertheless, there is no doubt that under- and over-coordinated charged structural defects, VAP and/or IVAP-type centers, must play a key role.

Summary and conclusions

The mobile carrier species controlling the xerographic depletion discharge in a-Sb_xSe_{1-x} alloys are electrons. Thermal generation of free electrons in a-Sb_xSe_{1-x} is accompanied by the simultaneous formation of deeply trapped positive space charge. We find that antimony alloying progressively enhances the free electron thermal generation rate relative to the pure specimen.

As apparent from the large xerographic residual potentials for Sb_xSe_{1-x} alloys, the addition of Sb to a-Se seems to greatly increase the concentration of deep localized states within the mobility gap of the material.

The results indicate that in the long wavelength region (e.g. $\lambda \sim 600 \text{ nm}$) the photosensitivity for the a-Sb_xSe_{1-x} films is higher than for the pure selenium probably due to a greater quantum efficiency.

- A.I.Ward, J. Non-Cryst. Solids 4 (1970) 80.
4. M.Abkowitz and J.M.Markovics, Sol. State Commun. 44 (1982) 1431.
5. C.Wood, R.Mueller and L.R.Gilbert, J. Non-Cryst. Solids 12 (1973) 295.
6. M.H.El-Zaidia, A.El-Shafi, A.A.Ammar and M.Abo-Ghozala. Thermochemica Acta 116 (1987) 35.
7. F.V.Pirogov, J. Non-Cryst. Solids 114 (1989)76.
8. P.J.Warter, Appl. Opt. Suppl., 3 (1985) 65.
9. M.Abkowitz and R.C.Enck, Phys. Rev. B 27 (1983) 7402.
10. M.Itoh and K.Tanaka, Jpn. J. Appl. Phys. 34 (1995) 2216.
11. V.I.Mikla, J.Phys.: Condens. Matter 8 (1996) 429.

ВИВЧЕННЯ ПЕРЕНОСУ НОСІЇВ ЗАРЯДУ ТА ЇХ ЗАХОПЛЕННЯ В СПЛАВАХ Sb_xSe_{1-x}

В.І.Мікла, Ю.Ю. Надь, В.В.Мікла, О.В. Мателешко

Ужгородський державний університет, 294000, Ужгород, вул.Волошина, 54

Розглянуто вплив введення атомів Sb на електронні властивості некристалічного селену. Аналіз процесів захоплення фотоінжекттованих носіїв і термічної генерації вільних носіїв свідчать, що задані процеси контролюються електронними станами, локалізованими в щільності рухливості Sb_xSe_{1-x} . Встановлено, що концентрація цих станів зростає із збільшенням вмісту Sb .